BROADBAND ASYMMETRIC ACOUSTIC TRANSMISSION BASED ON AN ACOUSTIC PRISM AND ABSORPTIVE MATERIAL

Ailing Song, Tianning Chen and Xiaopeng Wang

Xi'an Jiaotong University, School of Mechanical Engineering and State Key Laboratory for Strength and Vibration of Mechanical Structures, Xi'an, Shaanxi, China
email: ailing_song@126.com, tnchen@mail.xjtu.edu.cn

Narrow bandwidth and complicated structures are the main disadvantages of the existing asymmetric acoustic transmission devices. In this paper, a simple broadband asymmetric acoustic transmission device composed of an acoustic prism and absorptive material is proposed and numerically investigated. The triangular acoustic prism is filled with xenon gas and can modulate the propagation direction of transmitted wave according to the generalized Snell's law. The absorptive material can completely absorb the incoming waves. The sound pressure field distributions, sound intensity distributions, and transmittance are calculated by using finite element method. The sound pressure field distributions show that asymmetric acoustic transmission can be realized by the proposed device, which agree well with the theoretical predictions. The acoustic wave of left incidence is transmitted by the acoustic prism with a certain refraction angle and then the transmitted wave is absorbed by the absorptive material, the acoustic propagation is not allowed. However, the acoustic wave of right incidence can pass through the device due to the absence of absorptive material. The asymmetric acoustic transmission is valid within a remarkably broad frequency range from 1000 Hz to 10000 Hz. Besides, the effects of prism angle on the transmitted wave direction are discussed. The proposed device may have potential applications in various areas, such as medical ultrasound and noise control.
Keywords: asymmetric acoustic transmission, acoustic prism, absorptive material, broad frequency range

1. Introduction

The electric diodes can realize the rectification of current flux and bring significant revolutions in various fields [1]. Inspired by the electric diodes, some researchers have dedicated to investigating the asymmetric transmission of other forms of energy, such as optical energy [2], thermal energy [3], and acoustic energy [4-17]. The asymmetric acoustic transmission (AAT) device can realize the asymmetric transmission of acoustic waves. Recently, the AAT device has gradually become a research focus due to its potential applications in many areas, such as medical ultrasound and noise control.

In the beginning, the AAT devices were designed by breaking the time-reversal symmetry. Liang et al. [4,5] designed an AAT device by using a superlattice and a strongly nonlinear medium, and the acoustic energy rectification was demonstrated theoretically and experimentally. The nonlinear AAT devices can change the frequencies of acoustic waves, and have disadvantages of low conversion efficiency and complexity in experimental realization. Compared with the nonlinear AAT devices, the linear AAT devices that break the spatial reversal symmetry have attracted more attentions due to their significantly improved performances. The asymmetric grating structure can be used to design AAT devices based on one-way diffraction principle [6,7,8]. Phononic crystals (PCs) are periodic composites composed of two or more materials [9], and have been very important in realizing the AAT devices. Li et al. [10] experimentally demonstrated the asymmetric acoustic transmission in a PC-based AAT device that breaks the spatial reversal symmetry. Yuan et al. [11] and Song et al. [12] realized AAT devices composed of a bended waveguide and a linear PC. In recent years, the acoustic metasurface (AMS) has attracted extensive attentions and shows special advantages in the design of AAT devices. Li et al. [13] designed an acoustic prism composed of metamaterials with near-zero refractive index to realize high efficient asymmetric acoustic transmission. Zhu et al. [14,15] proposed two kinds of open tunnels by using reflective AMSs. Wang et al. [16] proposed an AAT device by using two structured impedance-matched AMSs. Song et al. [17] proposed a waveform-preserved AAT device composed of an AMS and a PC structure.

Although various AAT devices have realized asymmetric acoustic transmission in many literatures, most devices have complicated structures and the valid bandwidth is limited, which will restrict the potential applications of AAT device. In this research, we propose a simple AAT device by using an acoustic prism and absorptive material. Compared with the previous AAT devices, the proposed AAT device can realize asymmetric acoustic transmission within a broad frequency range. The acoustic prism is designed according to the generalized Snell's law. The sound pressure field distributions, the sound intensity field distributions, and the transmittance are calculated for different incident directions. Furthermore, the prism angle effects on transmitted wave directions are discussed. Finally, a brief conclusion is given.

2. Asymmetric acoustic transmission device

In this paper, a simple broadband AAT device is proposed by using an acoustic prism and absorptive material. The schematic of the proposed AAT device is shown in Fig. 1. The cross-section of the acoustic prism is right triangle (marked with "ABC" in Fig. 1), and the prism angle is denoted as θ. The prism is filled with xenon gas and placed in air, and the directions of the transmitted waves can be modulated according to the generalized Snell's law. The absorptive material is placed on the right of the acoustic prism (marked with "CD" in Fig. 1) and can completely absorb the incident waves. The absorptive material can be realized by metamaterials [18-20] or traditional materials, such as porous, spongy or fiber materials. Other boundaries are hard boundaries which can completely reflect the incident waves. In Fig. 1, the red and blue arrows denote the directions of the incident waves for left incidence (LI) and right incidence (RI), respectively. The sound velocities in air and xenon are c_A=343 m/s, c_X = 169 m/s, respectively. The acoustic impedances of air and xenon are Z_A=442.5 Pa s/m, Z_X= 996.1 Pa s/m, respectively. Besides, the interfaces between air and xenon can be separated by polyethelene films in the experiment [5]. Due to the impedances of air and xenon are in the same orders of magnitude, the proposed AAT device can achieve very high transmittance.

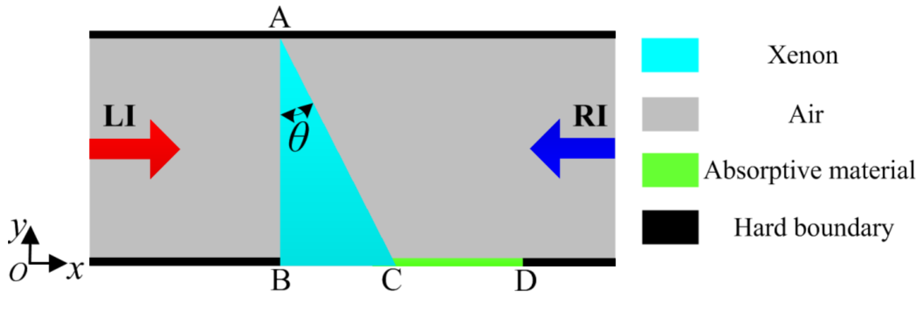

Figure 1: Schematic of the proposed AAT device.

First of all, it is necessary to clarify how the asymmetric acoustic transmission is realized by the proposed device. When the plane waves are incident from different directions, the wave paths represented by red arrow lines are shown in Fig. 2. In Fig. 2(a), the plane wave of LI is normally incident on the boundary "AB" and passes through the interface without changing the wave direction. Then the wave impinges on the boundary "AC" with incident angle θ_{i1}, and then transmits through the interface with refraction angle θ_{t1}. The direction of transmitted wave for LI case can be denoted by α. Finally, the transmitted wave is incident on the absorptive material and completely absorbed, so the acoustic propagation for LI case is forbidden. However, as shown in Fig. 2(b), the plane wave of RI can transmits through the acoustic prism and then impinges on the hard boundary, so the acoustic propagation for RI case is allowed due to the absence of absorptive material on the left. The direction of transmitted wave for RI case can be denoted by θ_{t3}. Therefore, the designed device can realize asymmetric acoustic transmission.

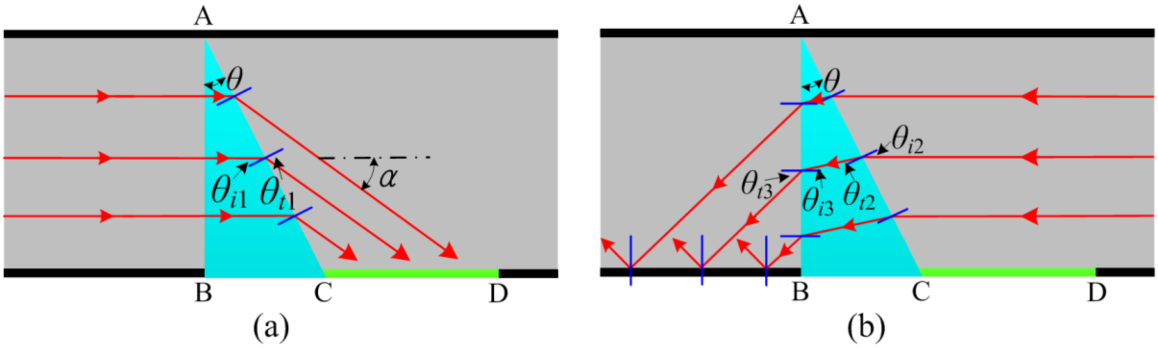

Figure 2: Schematics of the wave paths when the plane waves are incident from (a) left and (b) right.

It's important to point out that the prism angle θ should be carefully designed in order to realize the asymmetric acoustic transmission. When the plane wave is incident upon the interface between two media with different refractive index, the refraction will appear and obey the generalized Snell's law:

$$\sin(\theta_i)\cdot n_i = \sin(\theta_t)\cdot n_t . \quad (1)$$

where θ_i is the incident angle, θ_t is the refraction angle, n_i is the refractive index of incident medium, n_t is the refractive index of transmitted medium.

The refractive indexs of air and xenon are n_A=1, n_X= 2.03, respectively. When the acoustic wave is incident from xenon into air, the incident angle is smaller than the refraction angle and the critical angle for total reflection is $\theta_c= \sin^{-1}(c_X/c_A)$=29.5°. For LI case, at interface AC, the incident angle is $\theta_{i1}=\theta$, the refraction angle is $\theta_{t1}=\sin^{-1}(\sin(\theta_{i1})\cdot n_X/n_A)$. To ensure the total reflection does not occur at interface AC, the incident angle needs to satisfy $\theta_{i1}<\theta_c$. For RI case, at interface AC, the incident angle is $\theta_{i2}=\theta$, the refraction angle is $\theta_{t2}=\sin^{-1}(\sin(\theta_{i2})\cdot n_A/n_X)$. At interface AB, the incident angle is $\theta_{i3}=\theta-\theta_{t2}$, the refraction angle is $\theta_{t3}=\sin^{-1}(\sin(\theta_{i3})\cdot n_X/n_A)$. To ensure the total reflection does not occur at interface AB, the incident angle needs to satisfy $\theta_{i3}<\theta_c$. Therefore, the prism angle should be smaller than 29.5° to ensure the asymmetric acoustic transmission can be realized by the proposed device. In this paper, the prism angle is θ=28.125°, the boundary AB=32 cm, CD=20 cm.

3. Numerical Results and Discussions

3.1 Asymmetric acoustic transmission performance

To intuitively show the asymmetric acoustic transmission performance of the proposed AAT device, the sound pressure field p and sound intensity field $|p|^2$ at 6 kHz (an arbitrary frequency) for LI and RI cases are calculated and numerically analysed, as shown in Fig. 3. The colour maps indicate the sound pressure values and sound intensity values. All numerical simulations are performed by Comsol Multiphysics software based on finite element method [21]. Fig. 3(a) and (b) are the sound pressure field distributions for LI and RI cases, respectively. Fig. 3(c) and (d) are the sound intensity field distributions for LI and RI cases, respectively.

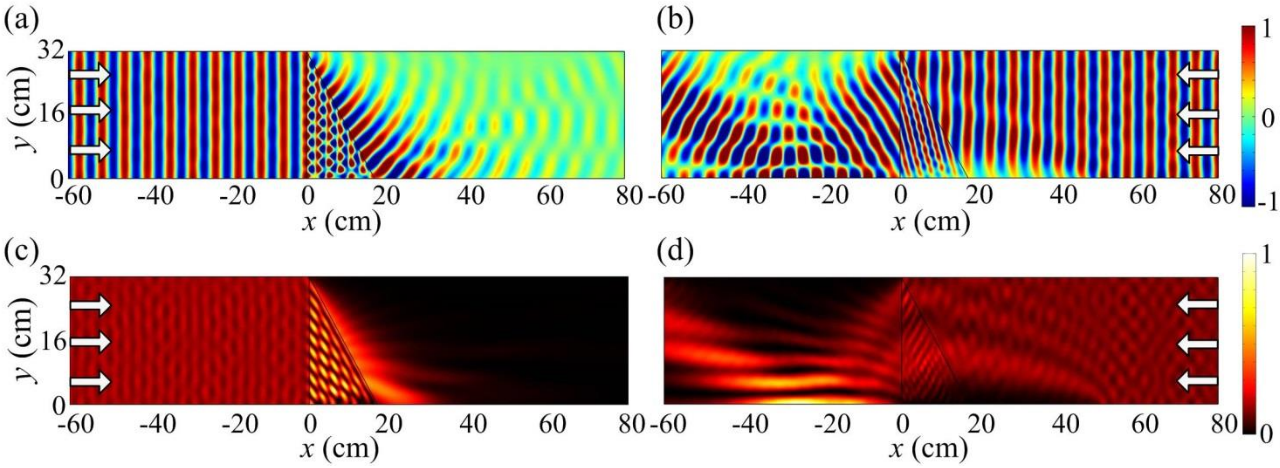

Figure 3: The sound pressure field distributions at 6 kHz for (a) LI and (b) RI cases. The sound intensity field distributions at 6 kHz for (c) LI and (d) RI cases. White arrows indicate the directions of the incident waves.

As shown in Fig. 3(a), the plane wave of LI transmits through the acoustic prism with refraction angle θ_{t1}=73.125°. Then the transmitted wave is completely absorbed by the absorptive material, so the acoustic propagation for LI case is forbidden. No sound intensity field distribution can be observed at the right side of the device, as shown in Fig. 3(c). For RI case, the plane wave passes through the acoustic prism with refraction angle θ_{t3}=31°, then impinges on the hard boundary with normal reflection as shown in Figs. 3(b). Therefore, the acoustic wave of RI can pass the proposed device. Besides, some sound intensity field distribution can be observed at the left side of the device, as shown in Fig. 3(d). The simulation results agree well with the theoretical predictions, which demonstrate that the proposed AAT device can realize asymmetric acoustic transmission. The asymmetric acoustic transmission is mainly attributed to the special design of prism angle and the usage of absorptive material.

3.2 Transmission spectra

In order to demonstrate the broadband performance of the designed device, the transmittance for LI (red solid line) and RI (blue solid line) cases are calculated and shown in Fig. 4. The transmittance is defined as the ratio of the transmitted power to the incident power. By changing the frequencies of acoustic waves from 0 kHz to 10 kHz, the transmission spectra of the proposed device are obtained.

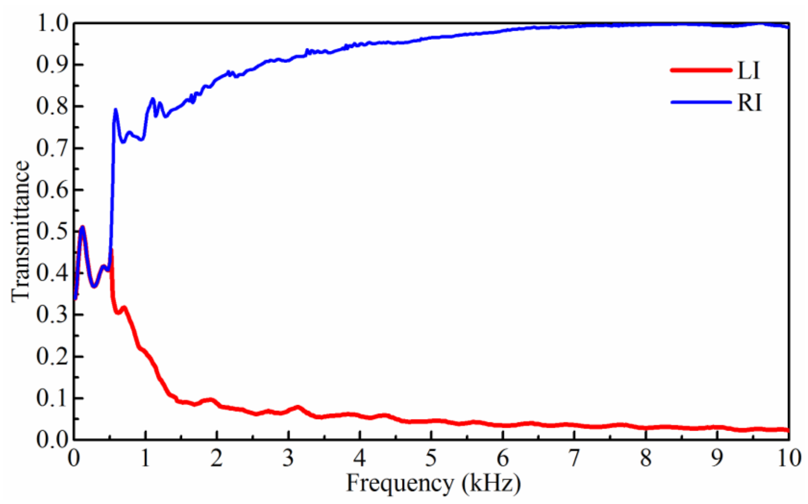

Figure 4: Transmission spectra of the proposed AAT device for LI and RI cases.

For the frequency range of 0–520 Hz, the transmission spectrum of LI case nearly overlaps with that of RI case, and the asymmetric acoustic transmission is invalid. This phenomenon is attributed to the wavelength of this frequency range is close to the prism size and the diffraction happens. When we increase the frequency to 520 Hz, the designed device begins to show asymmetric acoustic transmission performance. It is obvious that the transmittance of LI case decreases and that of RI case increases with the increase of frequency. For the frequency larger than 1000 Hz, the transmittance of LI case is less than 20%, and the transmittance of RI case is more than 70%. As we further increase the frequency to 2600 Hz, the transmittance of LI case is less than 10%, and the transmittance of RI case is more than 90%. What is more, the transmittance of RI case is almost 100% for the frequency larger than 7000 Hz. The results indicate that asymmetric acoustic transmission can be realized by the designed device within a broad bandwidth from 1000 Hz to 10000 Hz, which is a great advantage of the designed device. The broadband performance of the designed device is attributed to the wave paths are not affected by the frequencies. In other words, the wave paths are the same for incident waves of different frequencies. Actually, the designed device is still valid for frequencies larger than 10000 Hz.

3.3 Prism angle effects on the transmitted waves

As discussed earlier, the proposed device can realize asymmetric acoustic transmission if the prism angle is smaller than 29.5°. It is necessary to discuss the prism angle effects on the transmitted waves for both LI and RI cases. For LI case, the transmitted wave direction is denoted by α and can be expressed as $\alpha=\sin^{-1}(\sin(\theta)\cdot n_X/n_A)-\theta$ according to the generalized Snell's law. The relation between α and the prism angle θ is shown in Fig. 5(a). When we increase the prism angle from 0° to 29°, α is escalating faster and faster and increases from 0° to 50.8°. This means the transmitted waves of LI case gradually deviate from x axis with the increase of θ.

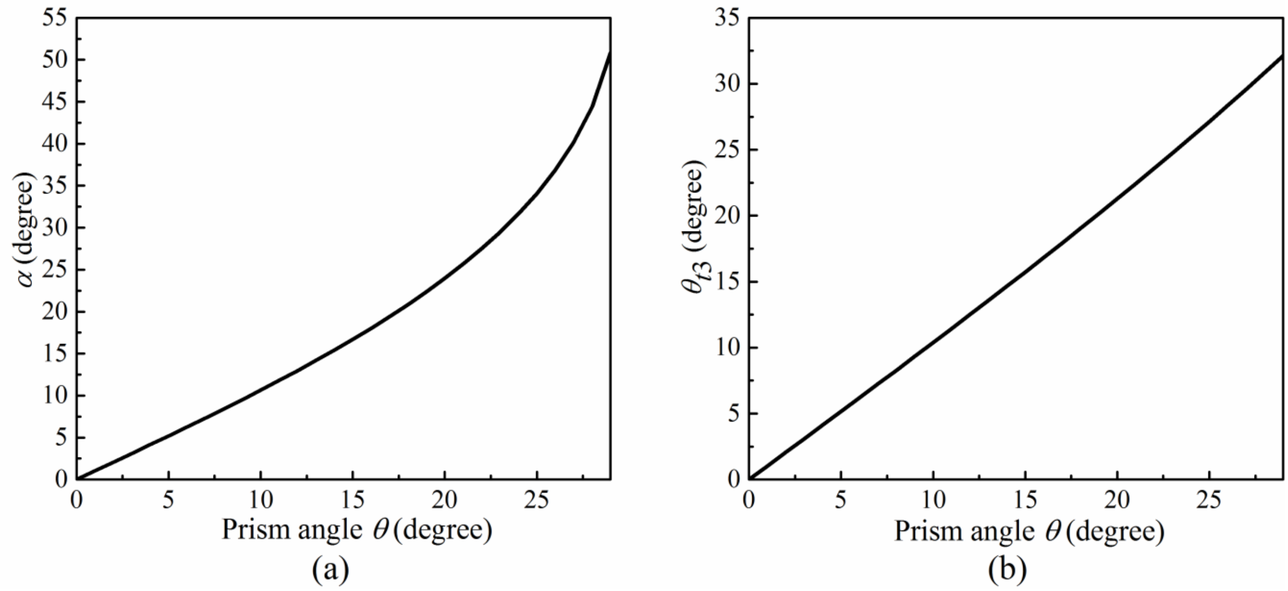

Figure 5: (a) The transmitted wave direction α as a function of the prism angle θ for LI case. (b) The transmitted wave direction θ_{t3} as a function of the prism angle θ for RI case.

Similarly, the transmitted wave direction of RI case is denoted by θ_{t3} and can be expressed as $\theta_{t3}=\sin^{-1}(\sin(\theta-\sin^{-1}(\sin(\theta)\cdot n_A/n_X))\cdot n_X/n_A)$ according to the generalized Snell's law. The relation between θ_{t3} and the prism angle θ is shown in Fig. 5(b), and is almost a linear relationship. It can be observed that θ_{t3} increases from 0° to 32.1° as we increase the prism angle from 0° to 29°. Increasing the prism angle can also result in the transmitted waves gradually deviate from x axis. From the above analysis, we can find that the designed acoustic prism can control the directions of the transmitted waves, and increase the prism angle can make the transmitted waves deviate from x axis for both LI and RI case.

4. Conclusions

In summary, we propose a simple broadband AAT device by using an acoustic prism and absorptive material. We first introduce the structure of the proposed AAT device. Then the acoustic prism filled with xenon gases is designed, and the prism angle should be smaller than 29.5 ° to ensure the proposed device can realize asymmetric acoustic transmission. The sound pressure field distributions and sound intensity field distributions show that the proposed device can realize asymmetric acoustic transmission, which agree well with the theoretical predictions. For LI case, the acoustic wave transmits through the acoustic prism and the transmitted wave is completely absorbed by the absorptive material, the acoustic propagation is forbidden. However, the acoustic wave of RI can pass through the device due to the absence of absorptive material. The transmission spectra show that the proposed AAT device is valid within a broad frequency range from 1000 Hz to 10000 Hz due to the wave paths are not affected by the wave frequencies. Finally, the prism angle effects on the transmitted wave directions for both LI and RI cases are discussed. The designed acoustic prism can modulate the directions of the transmitted waves, and increase the prism angle can make the transmitted waves deviate from x axis. The proposed broadband AAT device may have potential applications in many areas, such as medical ultrasound and noise control.

Acknowledgements

The authors gratefully acknowledge financial support from the Project of National Natural Science Foundation of China (Nos. 51275377 and 51675402), the National Basic Research Program of China (No. 2011CB610306), and the Collaborative Innovation Center of Suzhou Nano Science and Technology.

REFERENCES

1 Sinha, A. K. and Poate, J. M. Effect of alloying behavior on the electrical characteristics of n-GaAs Schottky diodes metallized with W, Au, and Pt, *Applied Physics Letters*, **23** (12), 666-668, (1973).

2 Scalora, M., Dowling, J. P., Bowden, C. M. and Bloemer, M. J. The photonic band edge optical diode, *Journal Applied Physics*, **76** (4), 2023-2026, (1994).

3 Boreyko, J. B., Zhao, Y. J. and Chen, C. H. Planar jumping-drop thermal diodes, *Applied Physics Letters*, **99** (23), 234105, (2011).

4 Liang, B., Yuan, B. and Cheng, J. C. Acoustic Diode: Rectification of acoustic energy flux in one-dimensional systems, *Physical Review Letters*, **103** (10), 104301, (2009).

5 Liang, B., Guo, X. S., Tu, J., Zhang, D. and Cheng, J. C. An acoustic rectifier, *Nature materials*, **9** (12), 989-992, (2010).

6 He, Z. J., Peng, S. S., Ye, Y. T., Dai, Z. W., Qiu, C. Y., Ke, M. Z. and Liu, Z. Y. Asymmetric acoustic gratings, *Applied Physics Letters*, **98** (8), 083505, (2011).

7 Sun, H. X., Zhang, S. Y. and Shui, X. J. A tunable acoustic diode made by a metal plate with periodical structure, *Applied Physics Letters*, **100** (10), 103507, (2012).

8 Li, Y., Tu, J., Liang, B., Guo, X. S., Zhang, D. and Cheng, J. C. Unidirectional acoustic transmission based on source pattern reconstruction, *Applied Physics Letters*, **112** (6), 064504, (2012).

9 Kushwaha, M. S., Halevi, P., Dobrzynski, L. and Djafari-Rouhani, B. Acoustic band structure of periodic elastic composites, *Physical Review Letters*, **71** (13), 2022-2025, (1993).

10 Li, X. F., Ni, X., Feng, L., Lu, M. H., He, C. and Chen,Y. F. Tunable unidirectional sound propagation through a sonic-crystal-based acoustic diode, *Physical Review Letters*, **106** (8), 084301, (2011).

11 Yuan, B., Liang, B., Tao, J. C., Zou, X. Y. and Cheng, J. C. Broadband directional acoustic waveguide with high efficiency, *Applied Physics Letters*, **101** (4), 043503, (2012).

12 Song, A. L., Chen, T. N., Wang, X. P. and Wan, L. L. Tunable broadband unidirectional acoustic transmission based on a waveguide with phononic crystal, *Applied Physics A*, **122** (8), 759, (2016).

13 Li, Y., Liang, B., Gu, Z. M., Zou, X. Y. and Cheng, J. C. Unidirectional acoustic transmission through a prism with near-zero refractive index, *Applied Physics Letters*, **103** (5), 053505, (2013).

14 Zhu, Y. F., Zou, X. Y., Liang, B. and Cheng, J. C. Broadband unidirectional transmission of sound in unblocked channel, *Applied Physics Letters*, **106** (17), 173508, (2015).

15 Zhu, Y. F., Zou, X. Y., Liang, B. and Cheng, J. C. Acoustic one-way open tunnel by using metasurface, *Applied Physics Letters*, **107** (11), 113501, (2015).

16 Wang, X. P., Wan, L. L., Chen, T. N., Liang, Q. X. and Song, A. L. Broadband acoustic diode by using two structured impedance-matched acoustic metasurfaces, *Applied Physics Letters*, **109** (4), 044102, (2016).

17 Song, A. L., Chen, T. N., Wang, X. P. and Wan, L. L. Waveform-preserved unidirectional acoustic transmission based on impedance-matched acoustic metasurface and phononic crystal, *Journal Applied Physics*, **120** (8), 085106, (2016).

18 Li, R. Q., Zhu, X. F., Liang, B., Li, Y., Zou, X. Y. and Cheng, J. C. A broadband acoustic omnidirectional absorber comprising positive-index materials, *Applied Physics Letters*, **99** (19), 193507, (2011).

19 Climente, A., Torrent, D. and Sánchez-Dehesa, J. Omnidirectional broadband acoustic absorber based on metamaterials, *Applied Physics Letters*, **100** (14), 144103, (2012).

20 Mei, J., Ma, G. C., Yang, M., Yang, Z. Y., Wen, W. J. and Sheng, P. Dark acoustic metamaterials as super absorbers for low-frequency sound, *Nature communications*, **3**, 756, (2012).

21 COMSOL Multiphysics, COMSOL Multiphysics User Guide (Version 4.3a), COMSOL AB, (2012).